J|A|C|S
ARTICLES
Published on Web 03/23/2007

PRODAN-Conjugated DNA: Synthesis and Photochemical Properties

Kazuki Tainaka,[†] Kazuo Tanaka,[†] Shuji Ikeda,[†] Ken-ichiro Nishiza,[‡] Tomo Unzai,[‡] Yoshimasa Fujiwara,[‡] Isao Saito,[§] and Akimitsu Okamoto*[,†,‡]

Contribution from the Frontier Research System, RIKEN (The Institute of Physical and Chemical Research), Wako, Saitama 351-1098, Japan, Department of Synthetic Chemistry and Biological Chemistry, Faculty of Engineering, Kyoto University, Kyoto 615-8510, Japan, and NEWCAT Institute, School of Engineering, Nihon University, and SORST, Japan Science and Technology Agency, Tamura, Koriyama 963-8642, Japan

Received December 21, 2006; E-mail: aki-okamoto@riken.jp

Abstract: A solvatochromic fluorophore, PRODAN, has been used as a microenvironment-sensitive reporter. Based on the chemistry of PRODAN, we designed and synthesized four novel fluorescent nucleosides, ^{PDN}X (X = U, C, A, and G), to which a PRODAN fluorophore was attached at pyrimidine C5 or purine C8. The fluorescent nucleosides sensitively varied the Stokes shift values depending on the orientational polarizability of the solvent. The ^{PDN}X incorporated into DNA also changed the Stokes shift values depending on the DNA structure. In particular, the excitation spectrum of the ^{PDN}X-containing duplex shifted to a longer wavelength and gave a smaller Stokes shift value when the base opposite ^{PDN}X could form a Watson−Crick base pair with ^{PDN}X. A lower energy excitation of ^{PDN}X-containing DNA resulted in a strong fluorescence emission selective to the Watson−Crick pairing base. This unique photochemical character was applicable to the efficient typing of single-nucleotide polymorphisms of genes.

Introduction

Local variations in the structure and dynamics of biomolecules play important roles in mediating the interactions between biomolecules. In particular, monitoring the microenvironmental change in conformation, polarity, viscosity, and charge around the DNA surface is essential in order to understand the great variety of biological events involving DNA in cells. For such a purpose, fluorescent probes that can be site-specifically incorporated into the DNA sequence of interest and are sensitive to the change in its microenvironment are highly valuable and desirable.[1] Nucleosides possessing various fluorophores have been explored to study the structures and dynamics of nucleic acids, including fluorescent nucleoside analogues, as exemplified by 2-aminopurine,[2] ethynyl-extended nucleobase derivatives,[3] and nucleoside analogues replaced by flat aromatic fluorophores.[4]

Solvatochromic fluorophores, which show shifts in absorption and emission bands induced by a change in solvent nature or composition, may be applicable to monitoring the structural transformation and intermolecular interaction of biomolecules with micropolarity change in the surroundings.[5] The most important fluorescent characteristic of a solvatochromic fluorophore is the linear correlation between the Stokes shifts of the fluorophores and the orientational polarizabilities of the solvents, based on the dipole interaction theory of Lippert and Mataga.[6] The well-known solvatochromic fluorophore 6-propionyl-2-dimethylaminonaphthalene (PRODAN) and its derivatives are among the most promising candidates for such a microenvironment-sensitive fluorescent probe.[7] The electronic transitions

[†] RIKEN (The Institute of Physical and Chemical Research).
[‡] Kyoto University.
[§] Nihon University and SORST, Japan Science and Technology Agency.

(1) (a) Wojczewski, C.; Stolze, K.; Engels, J. W. *Synlett* **1999**, 1667−1678. (b) Hawkins, M. E. *Cell Biochem. Biophys.* **2001**, *34*, 257−281.
(2) (a) Ward, D. C.; Reich, E.; Stryer, L. *J. Biol. Chem.* **1969**, *244*, 1228−1237. (b) Menger, M.; Tuschl, T.; Eckstein, F.; Porschke, D. *Biochemistry* **1996**, *35*, 14710−14716. (c) Lacourciere, K. A.; Stivers, J. T.; Marino, J. P. *Biochemistry* **2000**, *39*, 5630−5641. (d) Kimura, T.; Kawai, K.; Fujitsuka, M.; Majima, T. *Chem. Commun.* **2004**, 1438−1439. (e) Tashiro, R.; Sugiyama, H. *J. Am. Chem. Soc.* **2005**, *127*, 2094−2097.
(3) (a) Seela, F.; Zulauf, M.; Sauer, M.; Deimel, M. *Helv. Chim. Acta* **2000**, *83*, 910−927. (b) Hurley, D. J.; Seaman, S. E.; Mazura, J. C.; Tor, Y. *Org. Lett.* **2002**, *4*, 2305−2308. (c) Okamoto, A.; Kanatani, K.; Saito, I. *J. Am. Chem. Soc.* **2004**, *126*, 4820−4827. (d) Hwang, G. T.; Seo, Y. J.; Kim, S. J.; Kim, B. H. *Tetrahedron Lett.* **2004**, *45*, 3543−3546. (e) Saito, Y.; Miyauchi, Y.; Okamoto, A.; Saito, I. *Chem. Commun.* **2004**, 1704−1705, (f) Okamoto, A.; Tainaka, K.; Saito, I. *Bioconjugate Chem.* **2005**, *16*, 1105−1111. (g) Wagner, C.; Rist, M.; Mayer-Enthart, E.; Wagenknecht, H. A. *Org. Biomol. Chem.* **2005**, *3*, 2062−2063.
(4) (a) Strässler, C.; Davis, N. E.; Kool, E. T. *Helv. Chim. Acta* **1999**, *82*, 2160−2171. (b) Arzumanov, A.; Godde, F.; Moreau, S.; Toulmé, J.-J.; Weeds, A.; Gait, M. J. *Helv. Chim. Acta* **2000**, *83*, 1424−1436. (c) Kool, E. T. *Acc. Chem. Res.* **2002**, *35*, 936−943. (d) Okamoto, A.; Tainaka, K.; Saito, I. *J. Am. Chem. Soc.* **2003**, *125*, 4972−4973. (e) Okamoto, A.; Tainaka, K.; Saito, I. *Tetrahedron Lett.* **2003**, *44*, 6871−6874. (f) Okamoto, A.; Tainaka, K.; Saito, I. *Chem. Lett.* **2003**, *32*, 684−685. (g) Gaied, N. B.; Glasser, N.; Ramalanjaona, N.; Beltz, H.; Wolff, P.; Marquet, R.; Burger, A.; Mély, Y. *Nucleic Acids Res.* **2005**, *33*, 1031−1039. (h) Okamoto, A.; Tainaka, K.; Fujiwara, Y. *J. Org. Chem.* **2006**, *71*, 3592−3598.
(5) (a) Okamoto, A.; Tanaka, K.; Fukuta, T.; Saito, I. *J. Am. Chem. Soc.* **2003**, *125*, 9296−9297. (b) Jadhav, V. R.; Barawkar, D. A.; Ganesh, K. N. *J. Phys. Chem. B* **1999**, *103*, 7383−7385. (c) Kimura, K.; Kawai, K.; Majima, T. *Org. Lett.* **2005**, *7*, 5829−5832.
(6) (a) Lippert, E. Z. *Electrochem.* **1957**, *61*, 962−975. (b) Mataga, N.; Kaifu, Y.; Koizumi, M. *Bull. Chem. Soc. Jpn.* **1956**, *29*, 465−470.
(7) (a) Weber, G.; Farris, F. J. *Biochemistry* **1979**, *18*, 3075−3078. (b) MacGregor, R. B.; Weber, G. *Ann. N.Y. Acad. Sci.* **1981**, *366*, 140−154. (c) Prendergast, F. G.; Meyer, M.; Carlson, G. L.; Iida, S.; Potter, J. D. *J. Biol. Chem.* **1983**, *258*, 7541−7544. (d) MacGregor, R. B.; Weber, G. *Nature* **1986**, *319*, 70−73.

10.1021/ja069156a CCC: $37.00

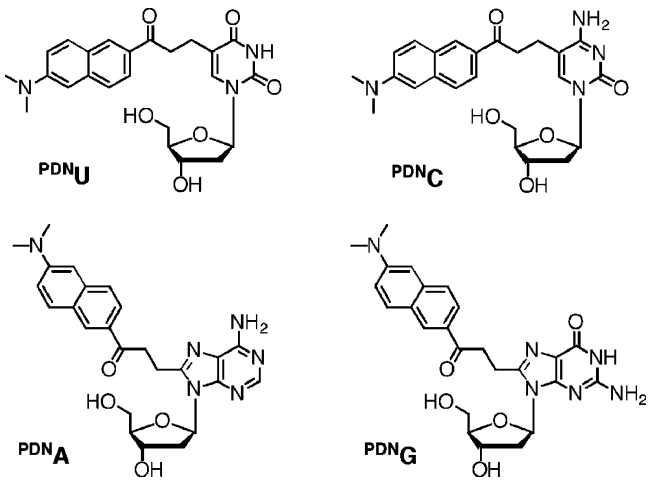

Figure 1. Structure of PRODAN-labeled nucleosides ^{PDN}X.

of PRODAN derivatives are strongly influenced by heterogeneous environmental factors in contact with the chromophore in the ground state.[8]

The inside of the grooves of the DNA helix is more hydrophobic than bulk water, and electron-rich heteroatoms of the natural bases are exposed to the surface of the major groove.[9] We presumed that a heterogeneous environmental change at a specific site of DNA could be read out as fluorescent signals if the PRODAN is anchored to the surface of the major groove. Therefore, we have designed novel fluorescent nucleosides possessing structures such that PRODAN is located at the surface of the major groove of the duplex.

In this paper, we report the synthesis of a new type of PRODAN-labeled nucleoside (^{PDN}X, X = U, C, A, and G) and the photochemical properties of oligodeoxyribonucleotides (ODNs) containing them (Figure 1). ^{PDN}X incorporated into DNA exhibited unique photochemical behavior in sensitive response to the nature of the complementary base of ^{PDN}X. The shift of the excitation spectra of PRODAN as a function of the base opposite ^{PDN}X resulted in the base-selective fluorescence emission by PRODAN as the result of lower energy excitation. This unique photochemical character is applicable to the efficient typing of single-nucleotide polymorphisms in genes.

Results and Discussion

Synthesis and Photochemical Properties of ^{PDN}U Nucleoside. Synthesis of the novel deoxyuridine-based fluorescent nucleoside is outlined in Scheme 1. 6-Dimethylamino-2-naphthaldehyde **1** was prepared according to the method reported in the literature.[10] Addition of lithium acetylide to **1** provided the corresponding coupling product, which was subsequently deprotected with sodium methoxide to give **2**. A 3′,5′-protected 5-iodo-2′-deoxyuridine was condensed with **2** to yield compound **3** via Sonogashira coupling. Hydrogenation of **3** followed by oxidation with tetrapropylammonium perruthenate produced **4**, which was then desilylated to afford the free nucleoside **5** (^{PDN}U).

We initially examined the photochemical properties of ^{PDN}U nucleoside **5** in different solvents. The fluorescence excitation spectra shifted depending on the nature of the solvent (Figure 2a and Table 1). From molecular orbital calculations, the first absorption band of PRODAN has been characterized by three different electronic transitions.[11] Excitation bands around 360 and 380 nm of ^{PDN}U correspond to the $\pi^* \rightarrow \pi$ transition and the $\pi^* \rightarrow n$ transition, respectively. The higher energy band predominates in nonpolar solvents, whereas the lower energy band contributes progressively more to the excitation spectra in protic solvents. These spectral changes can be attributed to specific interactions, such as hydrogen bonds, between ^{PDN}U and solvent molecules. A series of emission spectra showed solvent-dependent shifts of the fluorescence emission. Thus, the Stokes shift, the difference in wavenumbers between excitation maximum and emission maximum, greatly changed with solvent polarity (Figure 2b and Table 1). The change in the Stokes shift ($\Delta\nu$) was roughly proportional to the orientational polarizability (Δf) of the solvent, obeying the dipole interaction theory of Lippert and Mataga (Figure 2c).[6] ^{PDN}U in protic solvents showed a larger solvatochromic shift, suggesting the existence of specific solute−solvent interactions, such as hydrogen bonding.[12] Such solvatochromic behavior of ^{PDN}U would make possible the fluorometric detection of the microstructural changes in DNA through incorporation of ^{PDN}U into DNA and subsequent monitoring of the photochemical behavior.

Scheme 1 [a]

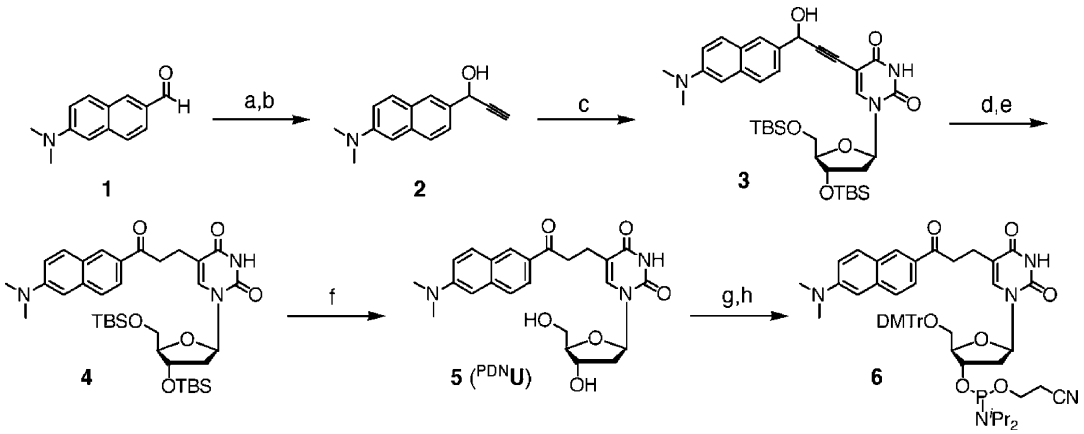

[a] Reagents and conditions: (a) trimethylsilylacetylene, 1.6 M *n*-BuLi, THF, −78 °C, 30 min, 92%; (b) 0.1 M sodium methoxide, methanol, room temperature, 1 h, 97%; (c) 5-iodo-3′*O*,5′*O*-bis(*tert*-butyldimethylsilyl)-2′-deoxyuridine, tetrakis(triphenylphosphine)palladium(0), copper(I) iodide, triethylamine, DMF, room temperature, 5 h, 93%; (d) 10% Pd/C, methanol, H_2, room temperature, 9 h, 72%; (e) tetrapropylammonium perruthenate, 4-methylmorpholine *N*-oxide, 4 Å MS, dichloromethane, room temperature, 1 h, 85%; (f) 1 M tetrabutylammonium fluoride, room temperature, 12 h, 82%; (g) 4,4′-dimethoxytrityl chloride, pyridine, room temperature, 4 h, 93%; (h) $(^{i}Pr_2N)_2PO(CH_2)_2CN$, 1*H*-tetrazole, acetonitrile, room temperature, 30 min.

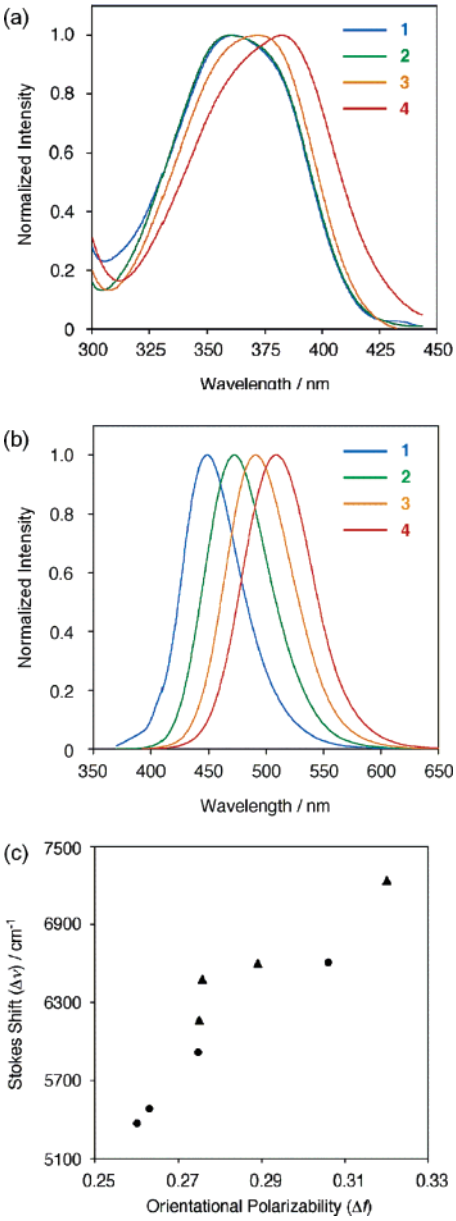

Figure 2. Photochemical behavior of ^{PDN}U nucleoside **5**. (a) Normalized excitation spectra in different solvents. Signal 1, HMPA; signal 2, acetonitrile; signal 3, ethanol; signal 4, ethylene glycol. (b) Normalized emission spectra in different solvents. Signal 1, HMPA; signal 2, acetonitrile; signal 3, ethanol; signal 4, ethylene glycol. (c) Lippert plot of Stokes shift in wavenumbers ($\Delta\nu$) against the orientational polarizability (Δf) of aprotic (●) and protic (▲) solvents.

Photochemistry of ^{PDN}U-Containing DNA. ^{PDN}U nucleoside **5** was incorporated efficiently into an ODN according to a conventional phosphoramidite method after protection of **5** and conversion into the phosphoramidite form **6** (Scheme 1). We examined the photochemical properties of the single-stranded **ODN1(^{PDN}U)**, 5′-d(CGCAAC^{PDN}UCAACGC)-3′, and the duplex formed by hybridization with **ODN1′(A)**, 5′-d(GCGTTGAGTTGCG)-3′ (Table 2). Excitation maxima of ^{PDN}U were observed at 380 nm in the free nucleoside, at 389 nm in single-stranded ODN, and at 404 nm in the duplex form. The excitation spectra of ^{PDN}U-containing ODNs compared with the free nucleoside ^{PDN}U in aqueous solution showed larger bathochromic shifts (Figure 3a and Table 3). The origin of the shift in the excitation spectra was ascribed to additional interactions between the chromophore and surroundings in the ground state in addition to interaction with water molecules. As described above, the higher energy band around 380 nm in the excitation spectra corresponds to the $\pi^* \rightarrow n$ transition with charge-transfer character. Previous reports have suggested that this electronic transition band might be greatly stabilized by interactions between the dimethylamino group or carbonyl group of the PRODAN chromophore and specific functional groups, such as ester linkage, ether linkage, hydroxy residue, and amide linkage.[8] In the duplex, the PRODAN chromophore that is attached to the uracil base at the C5 position via a short linker could be anchored to the vicinity of the surface in the major groove because of stable base pairing with an adenine base. The bathochromic shift of the excitation spectra in the fully matched duplex might originate from the electronic interactions between the PRODAN chromophore and the heteroatoms exposed on the surface of the DNA duplex. Although ^{PDN}U in the single strand would also interact with the heteroatoms of the DNA bases, a smaller bathochromic effect could result because of the lack of a tight interaction by effective interchain diffusion in the single-stranded state. The emission maxima of the free nucleoside, the single-stranded **ODN1(^{PDN}U)**, and the

Table 1. Photochemical Properties of ^{PDN}U Nucleoside **5** in Different Solvents[a]

solvents	$\lambda_{ex.max}$ (nm)	$\lambda_{em.max}$ (nm)	Φ_F	$\Delta\nu$ (cm^{-1})	Δf [b]
		aprotic			
HMPA	362	449	0.553	5373	0.260
DMSO	371	465	0.413	5487	0.265
DMF	363	462	0.361	5918	0.275
acetonitrile	360	472	0.417	6609	0.306
		protic			
2-propanol	371	481	0.325	6164	0.275
glycol	382	508	0.168	6479	0.276
ethanol	371	491	0.281	6600	0.289
water	380	524	0.033	7238	0.320

[a] Conditions: 2.5 μM ^{PDN}U nucleoside **5** in different solvents at 25 °C. [b] Orientational polarizabilitiy (Δf) is defined by $\Delta f = (\epsilon - 1)/(2\epsilon + 1) - (n^2 - 1)/(2n^2 + 1)$.

Table 2. ODNs Used in This Study

	sequences
ODN1(^{PDN}U)	5′-d(CGCAAC^{PDN}UCAACGC)-3′
ODN1(^{PDN}C)	5′-d(CGCAAC^{PDN}CCAACGC)-3′
ODN1(^{PDN}A)	5′-d(CGCAAC^{PDN}ACAACGC)-3′
ODN1(^{PDN}G)	5′-d(CGCAAC^{PDN}GCAACGC)-3′
ODN1′(N) (**N** = A, G, T, or C)	5′-d(GCGTTGNGTTGCG)-3′
ODN2(^{PDN}U)	5′-d(CGCAAT^{PDN}UTAACGC)-3′
ODN2′(N) (**N** = A, G, T, or C)	5′-d(GCGTTANATTGCG)-3′
ODN$_{MTHFR}$(^{PDN}U)	5′-d(GAG^{PDN}UCGATTTCAT)-3′
ODN$_{MTHFR}$(^{Py}C)	5′-d(GAG^{Py}CCGATTTCAT)-3′

(8) (a) Viard, M.; Gallay, J.; Vincent, M.; Meyer, O.; Robert, B.; Paternostre, M. *Biophys. J.* **1997**, *73*, 2221−2234. (b) Parasassi, T.; Krasnowska, E. K.; Bagatolli, L.; Gratton, E. *J. Fluorescence* **1998**, *8*, 365−373. (c) Bagatolli, L. A.; Parasassi, T.; Fidelio, G. D.; Gratton, E. *Photochem. Photobiol.* **1999**, *70*, 557−564. (d) Sire, O.; Alpert, B.; Royer, C. A. *Biophys. J.* **1996**, *70*, 2903−2914.
(9) (a) Lamm, G.; Pack, G. R. *J. Phys. Chem.* **1997**, *101*, 959−965. (b) Young, M. A.; Jayaram, B.; Beveridge, D. L. *J. Phys. Chem. B* **1998**, *102*, 7666−7669.
(10) List, B.; Barbas, C. F., III; Lerner, R. A. *Proc. Natl. Acad. Sci. U.S.A.* **1998**, *95*, 15351−15355.
(11) Ilich, P.; Prendergast, F. G. *J. Phys. Chem.* **1989**, *93*, 4441−4447.
(12) (a) Jozefowicz, M.; Kozyra, K. A.; Heldt, J. R.; Heldt, J. *Chem. Phys.* **2005**, *320*, 45−53. (b) Zurawsky, W. P.; Scarlata, S. F. *J. Phys. Chem.* **1992**, *96*, 6012−6016.

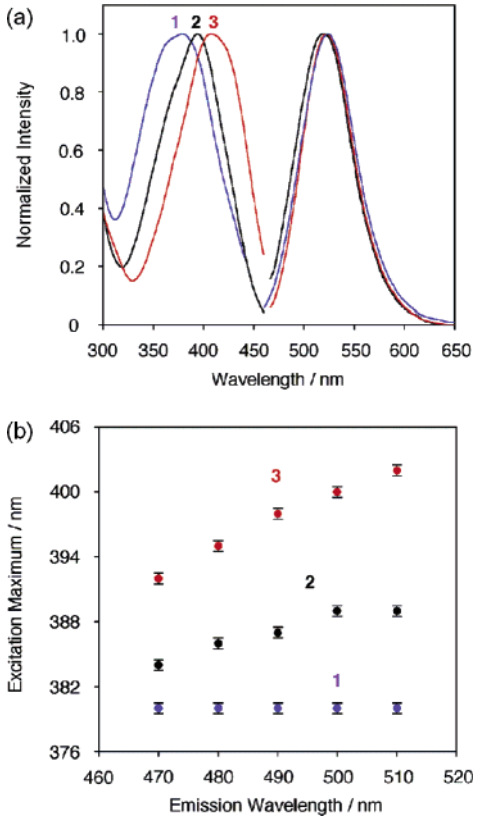

Figure 3. Comparison of the fluorescence excitation and emission spectra of ^{PDN}U nucleoside, ^{PDN}U in a single-stranded DNA, and ^{PDN}U in a duplex DNA. (a) Fluorescence excitation (left) and emission (right) spectra of nucleoside **5** (1, blue), single-stranded (2, black), and duplex (3, red). Excitation spectra were measured for emission at a wavelength of 520 nm, and emission spectra were excited at 380, 389, and 404 nm for nucleoside, single-stranded, and duplex, respectively. (b) Blue edge effect. Fluorescence excitation maxima of nucleoside **5** (1, blue), single-stranded (2, black), and duplex (3, red) are plotted against the emission wavelength at the blue edge of the fluorescence spectra.

duplex **ODN1(^{PDN}U)/ODN1′(A)** were observed at 524, 520, and 522 nm, respectively, and thus their Stokes shift values showed great variation, corresponding to 7238, 6476, and 5559 cm^{-1}, respectively. Smaller Stokes shifts might indicate that the position of the PRODAN chromophore would be restricted to the vicinity of the hydrophobic surface in the major groove. The restriction in mobility of the fluorophore upon binding to DNA gives rise to the viscosity effect in the photochemical properties.[13] In general, when the fluorophore positioned in rigid and viscous media can be stabilized by heterogeneous interactions with the surroundings in the ground state, the excitation spectra measured at the blue edge of the fluorescence signal is shifted to shorter wavelengths as a function of emission wavelength.[14] Figure 3b shows a plot of excitation maximum against each wavelength at the blue edge region of the fluorescence spectra. Excitation spectra of the ^{PDN}U nucleoside exhibited little change, whereas large bathochromic shifts of the excitation maximum were observed in the case of ^{PDN}U incorporated into DNA ($\Delta\lambda_{ex}$ = 5 nm in the single-stranded state, $\Delta\lambda_{ex}$ = 11 nm in the duplex). The dependence of excitation spectra on emission wavelength suggests that the photochemical behavior of the DNA-tethered chromophore would be affected by heterogeneous interactions not only with bulk water molecules but also with other factors, such as the identity of the heteroatoms of the DNA bases.

The effect on the Stokes shift of the heterogeneity in the microenvironment around ^{PDN}U may be increased by a large restriction in mobility due to stable base pair formation of ^{PDN}U incorporated into a fully matched duplex. Therefore, we assumed that when the complementary base of ^{PDN}U is a mismatched base (i.e., N = C, G, and T), an increase in the flexibility of ^{PDN}U due to the failure of base pairing would result in a decrease in heterogeneous interactions. Before measuring the excitation and emission spectra, we examined the duplex stabilities of **ODN1(^{PDN}U)** hybridized with the complementary strand **ODN1′(N)** (N = A, C, G, or T) (Table 3). The melting temperature (T_m) of **ODN1(^{PDN}U)/ODN1′(A)** (60 °C) was close to the T_m of the "native" T/A duplex (61 °C), showing that the PRODAN-labeled DNA formed a thermally stable duplex. On the other hand, the T_m values observed for mismatched duplexes were 4 to 9 °C lower than that of **ODN1(^{PDN}U)/ODN1′(A)**, and the stability of mismatched duplexes decreased in the order N = G, T, and C of **ODN1′(N)**.

The destabilization of duplexes due to the failure of base pairing influenced the photochemical behavior of **ODN1(^{PDN}U)**. Measurements of the excitation spectra of 2.5 μM of the **ODN1(^{PDN}U)/ODN1′(N)** duplex in sodium phosphate buffer (pH = 7.0) were performed at the emission wavelength of 520 nm (Figure 4). The excitation spectra of the mismatched duplex were changed significantly by the nature of the complementary base. When the base opposite ^{PDN}U is C, G, and T, excitation maxima were observed at 390, 400, and 398 nm, respectively. These wavelengths were shorter than the excitation maximum of the matched duplex **ODN1(^{PDN}U)/ODN1′ (A)**. The unique spectral shifts in the excitation spectra are valuable for discrimination of the nature of the base located at the opposite site of ^{PDN}U by use of red-edge excitation. The absorbance of **ODN1(^{PDN}U)/ODN1′ (A)** at 450 nm was considerably larger than those of other duplexes. The fluorescence spectrum of **ODN1(^{PDN}U)/ODN1′(A)** exhibited a strong fluorescence at 522 nm on excitation at 450 nm (Φ_F = 0.201), whereas the fluorescence of single-stranded **ODN1(^{PDN}U)** and mismatched **ODN1(^{PDN}U)/ODN1′(N)** (N = C, G, or T) duplexes were much weaker (Figure 4). The emission maximum in mismatched duplexes was slightly affected by alteration of the complementary base of ^{PDN}U (λ_{em} = 518−521 nm), and based on these data, the Stokes shifts of mismatched duplexes were calculated as 6373, 5806, and 5858 cm^{-1} for N = C, G, and T, respectively. The Stokes shift increased with an increase in the thermal stability of the duplexes. This relationship indicates that the formation of a stable base pair may be correlated with the generation of interactions between the PRODAN of ^{PDN}U and heteroatoms of the groove surface affecting the decrease in Stokes shift.

The Stokes shift of ^{PDN}U varied greatly depending on the nature of the base opposite ^{PDN}U. On the other hand, the effect of the flanking base pair of ^{PDN}U on the Stokes shift was small. ODNs containing the −T^{PDN}UT− sequence, **ODN2(^{PDN}U)**, were prepared, and the fluorescence of duplexes hybridized with the complementary strand **ODN2′(N)** was measured. The photo-

(13) (a) Okamoto, A.; Tainaka, K.; Nishiza, K.-i.; Saito, I. *J. Am. Chem. Soc.* **2005**, *127*, 13128−13129. (b) Balter, A. *J. Fluorescence* **1997**, *7*, S99−105. (c) Bajorek, A.; Pączkowski, J. *Macromolecules* **1998**, *31*, 86−95.

(14) (a) Demchenko, A. P. *Luminescence* **2002**, *17*, 19−42. (b) Pavlovich, V. S. *Zh. Prikl. Spektr.* **1976**, *25*, 480−487.

Table 3. Photochemical Properties[a] and Melting Temperatures (T_m)[b] of ^{PDN}U-Containing ODNs

entry	ODN	$\lambda_{ex.\,max}$ (nm)	$\lambda_{em.\,max}$ (nm)	I_{rel}[c]	Φ_F	$\Delta\nu$ (cm^{-1})	T_m (°C)
1	**ODN1(^{PDN}U)**	389	520	0.273	0.179	6476	
2	**ODN1(^{PDN}U)/ODN1′(A)**	404	522	1	0.201	5559	60.0
3	**ODN1(^{PDN}U)/ODN1′(C)**	390	518	0.289	0.115	6373	50.7
4	**ODN1(^{PDN}U)/ODN1′(G)**	400	521	0.392	0.068	5806	56.3
5	**ODN1(^{PDN}U)/ODN1′(T)**	398	519	0.290	0.073	5858	53.5
6	**ODN2(^{PDN}U)**	389	517	0.243	0.077	6365	
7	**ODN2(^{PDN}U)/ODN2′(A)**	406	518	1	0.212	5326	50.6
8	**ODN2(^{PDN}U)/ODN2′(C)**	395	518	0.346	0.143	6011	42.7
9	**ODN2(^{PDN}U)/ODN2′(G)**	401	518	0.344	0.073	5634	46.1
10	**ODN2(^{PDN}U)/ODN2′(T)**	399	516	0.406	0.091	5689	45.9

[a] Conditions: The duplexes (2.5 μM) were measured in 50 mM sodium phosphate (pH = 7.0) and 0.1 M sodium chloride at 25 °C. [b]The absorbance of the samples was monitored at 260 nm from 10 to 90 °C. [c]Relative fluorescence intensities were monitored at 520 nm after excitation at 450 nm.

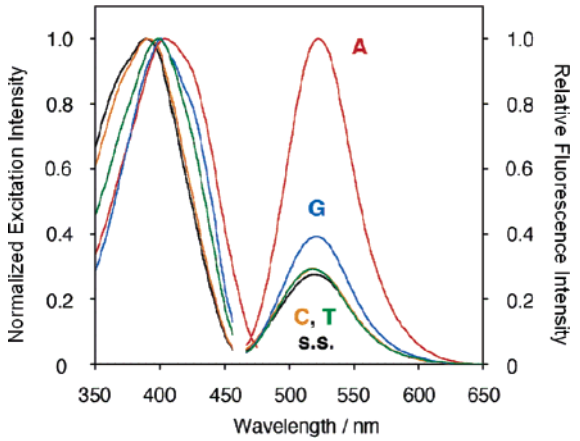

Figure 4. Fluorescence excitation and emission spectra of **ODN1(^{PDN}U)/ODN1′**(N). Normalized excitation (left) and relative emission (right) spectra of 2.5 μM **ODN1(^{PDN}U)** hybridized with 2.5 μM **ODN1′**(N) were measured in 50 mM sodium phosphate (pH = 7.0) and 0.1 M sodium chloride at 25 °C. "s.s." denotes a single-stranded **ODN1(^{PDN}U)**. Excitation spectra were measured for the 450 nm emission wavelength, and excitation spectra were measured for the 520 nm emission wavelength.

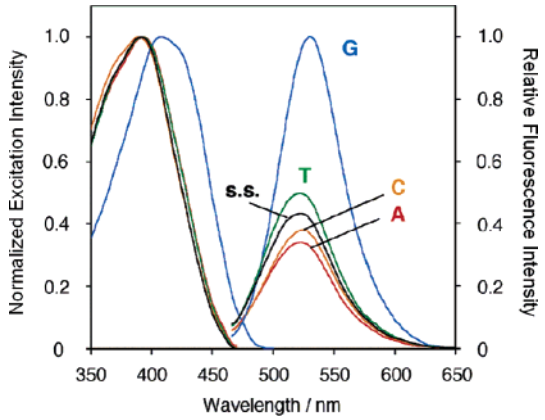

Figure 5. Fluorescence excitation and emission spectra of **ODN1(^{PDN}C)/ODN1′**(N). Normalized excitation (left) and relative emission (right) spectra of 2.5 μM **ODN1(^{PDN}C)** hybridized with 2.5 μM **ODN1′**(N) were measured in 50 mM sodium phosphate (pH = 7.0) and 0.1 M sodium chloride at 25 °C. "s.s." denotes a single-stranded **ODN1(^{PDN}C)**. Excitation spectra were measured for the 450 nm emission wavelength, and excitation spectra were measured for the 520 nm emission wavelength.

chemical properties of the duplexes are summarized in Table 3. The melting temperature of **ODN2(^{PDN}U)/ODN2′(A)** was 4 to 8 °C higher than those of mismatched duplexes. The higher thermal stability of the duplex was followed by the bathochromic shift of the excitation spectra and the decrease in the value of the Stokes shift in a similar fashion to the photochemical behavior observed for **ODN1(^{PDN}U)/ODN1′(A)**. The fluorescence intensity of the fully matched **ODN2(^{PDN}U)/ODN2′(A)** duplex was relatively high (Φ_F = 0.212) on excitation at 450 nm, whereas the fluorescence emissions of the single-stranded **ODN2(^{PDN}U)** and mismatched **ODN2(^{PDN}U)/ODN2′(N)** (N = C, G, or T) duplexes were suppressed. The fluorescence behavior of **ODN2(^{PDN}U)** suggests that the effect of the nature of the neighboring base pair on the photochemical behavior of ^{PDN}U is not significant.

Photochemistry of ^{PDN}C-Containing DNA. Because the novel fluorescent deoxyuridine ^{PDN}U displayed a sharp change in the Stokes shift in response to the nature of the complementary base, we assumed that the analogous C derivative (^{PDN}C) would also exhibit a complementary base-dependent Stokes shift change in a similar fashion as ^{PDN}U. The synthetic route for ^{PDN}C is outlined in Scheme S1 (Supporting Information). The fluorophore precursor **2** was coupled with 3′,5′-bissilyl-5-iodo-2′-deoxycytidine under Sonogashira coupling conditions to produce **7**. After hydrogenation of **7**, the C4 amino group of cytosine was protected by a formamidine group to yield **8**. Oxidation of **8** with tetrapropylammonium perruthenate produced PRODAN-labeled C derivative **9**. The protective group of **9** was converted from a labile formamidine group[15] to an acetyl group, which was subsequently desilylated to give **10**. The deoxyribose 5′-hydroxy group of **10** was protected with the 4,4′-dimethoxytrityl group, and then the resulting nucleoside was converted into the phosphoramidite **11**. The ^{PDN}C-containing ODN, **ODN1(^{PDN}C)**, was synthesized using **11**, and then the excitation and emission spectra of **ODN1(^{PDN}C)** hybridized with **ODN1′(N)** were measured (Figure 5). The excitation maxima of single-stranded **ODN1(^{PDN}C)** and mismatched duplexes were observed at 388−391 nm. On the other hand, the excitation maximum of **ODN1(^{PDN}C)/ODN1′(G)** was observed at 410 nm, a shift to a significantly longer wavelength of approximately 20 nm. In addition, the bathochromic effect on the excitation spectrum in a fully matched duplex resulted in the lowest value of Stokes shift ($\Delta\nu$ = 5522 cm^{-1}), while the Stokes shifts of other duplexes were calculated to be within the range 6491 to 6762 cm^{-1}. The melting temperature of **ODN1(^{PDN}C)/ODN1′(G)** was 9 to 11 °C higher than that of mismatched duplexes (Table 4), suggesting that the base pair stability affects the variation of Stokes shift through heterogeneous microenvironmental factors in contact with the PRODAN chromophore. The use of

(15) (a) Zemlicka, J.; Chládek, S.; Holy, A.; Smrt, J. *Collect. Czech. Chem. Commun.* **1966**, *31*, 3198−3211. (b) Vincent, S.; Mioskowski, C.; Lebeau, L. *J. Org. Chem.* **1999**, *64*, 991−997.

Table 4. Photochemical Properties[a] and Melting Temperatures (T_m)[b] of ^{PDN}X-Containing ODNs

entry	ODN	$\lambda_{ex.max}$ (nm)	$\lambda_{em.max}$ (nm)	I_{rel}[c]	Φ_F	$\Delta\nu$ (cm^{-1})	T_m(°C)
1	**ODN1(^{PDN}C)**	390	525	0.410	0.070	6593	
2	**ODN1(^{PDN}C)/ODN1′(A)**	391	525	0.328	0.053	6528	55.6
3	**ODN1(^{PDN}C)/ODN1′(C)**	388	526	0.365	0.055	6762	54.5
4	**ODN1(^{PDN}C)/ODN1′(G)**	410	530	1	0.077	5522	65.3
5	**ODN1(^{PDN}C)/ODN1′(T)**	391	524	0.471	0.065	6491	56.2
6	**ODN1(^{PDN}A)**	391	522	0.260	0.096	6418	
7	**ODN1(^{PDN}A)/ODN1′(A)**	382	526	0.179	0.080	7167	57.6
8	**ODN1(^{PDN}A)/ODN1′(C)**	394	526	0.322	0.069	6369	55.8
9	**ODN1(^{PDN}A)/ODN1′(G)**	397	522	0.664	0.167	6032	56.7
10	**ODN1(^{PDN}A)/ODN1′(T)**	405	517	1	0.202	5349	60.3
11	**ODN1(^{PDN}G)**	391	524	0.290	0.121	6491	
12	**ODN1(^{PDN}G)/ODN1′(A)**	373	515	0.167	0.072	7392	57.5
13	**ODN1(^{PDN}G)/ODN1′(C)**	406	519	1	0.128	5363	64.4
14	**ODN1(^{PDN}G)/ODN1′(G)**	381	521	0.191	0.097	7053	60.3
15	**ODN1(^{PDN}G)/ODN1′(T)**	398	524	0.750	0.113	6042	57.9

[a] Conditions: The duplexes (2.5 μM) were measured in 50 mM sodium phosphate (pH = 7.0) and 0.1 M sodium chloride at 25 °C. [b]The absorbance of the samples was monitored at 260 nm from 10 to 90 °C. [c]Relative fluorescence intensities were monitored at 520 nm after excitation at 450 nm.

excitation at a longer wavelength (λ_{ex} = 450 nm) gave a highly G-selective fluorescence emission from **ODN1(^{PDN}C)/ODN1′(N)** (Figure 5).

Photochemistry of ^{PDN}A- and ^{PDN}G-Containing DNA. PRODAN tethered to pyrimidine C6 resided in a duplex major groove and resulted in a base-selective decrease in the Stokes shift. Therefore, because substituents attached at the purine C8 position are placed at the side of the major groove, the purine derivatives, ^{PDN}A and ^{PDN}G, in which PRODAN was attached to the purine C8 position, should exhibit photochemical character in a similar fashion to those observed for ^{PDN}U and ^{PDN}C. These fluorescent purines were synthesized according to Scheme S2 (Supporting Information), and the fluorescence and thermal denaturation experiments were conducted under the conditions described above. The Stokes shifts of ^{PDN}A and ^{PDN}G were also significantly changed depending on the nature of the opposite base (Table 4 and Figure 6). The bathochromic effect on the excitation spectra in fully matched duplexes resulted in the lowest value of Stokes shift ($\Delta\nu$ = 5349 and 5363 cm^{-1} for ^{PDN}A and ^{PDN}G, respectively). On the other hand, the maxima of the excitation spectra and the Stokes shift values of mismatched duplexes varied widely. The **ODN1(^{PDN}A)/ODN1′(A)** and **ODN1(^{PDN}G)/ODN1′(A)** duplexes exhibited very large Stokes shifts, whereas the relatively small Stokes shifts of **ODN1(^{PDN}A)/ODN1′(G)** and **ODN1(^{PDN}G)/ODN1′(T)** showed significantly high fluorescence intensities on excitation at 450 nm. Substitution at purine C8 may induce the formation of wobble Watson−Crick base pairs or Hoogsteen base pairs by a conformational transition,[16] which modulates the interaction between the chromophore and the microenvironment factors.

Application to Multicolored Genotyping. These marked changes in the photochemical behavior of ^{PDN}X-containing DNAs that are dependent on the nature of the complementary base may play a key role in a facile genotyping assay. We have previously developed base-discriminating fluorescent nucleosides (BDF nucleosides) that change their fluorescence intensity depending on the nature of the nucleoside pairing with the BDF nucleoside.[3c,17] By hybridization of a probe containing a BDF nucleoside with a target DNA, the type of single-nucleotide polymorphism (SNP) base in the target DNA was fluorometrically identified with high accuracy. A DNA probe containing a typical BDF nucleoside ^{Py}C exhibits a strong fluorescence when a ^{Py}C/G base pair is formed by hybridization with a comple-

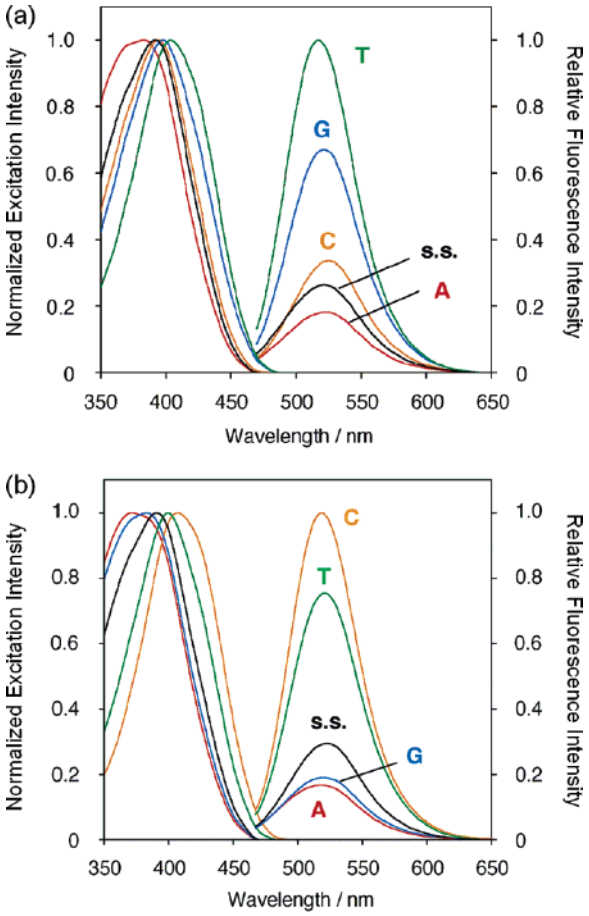

Figure 6. Fluorescence excitation and emission spectra of **ODN1(^{PDN}X)/ODN1′**(N) (X = (a) A and (b) G). Normalized excitation (left) and relative emission (right) spectra of 2.5 μM **ODN1(^{PDN}X)** hybridized with 2.5 μM **ODN1′**(N) were measured in 50 mM sodium phosphate (pH = 7.0) and 0.1 M sodium chloride at 25 °C. "s.s." denotes a single-stranded **ODN1(^{PDN}X)**. Excitation spectra were measured for the 450 nm emission wavelength, and excitation spectra were measured for the 520 nm emission wavelength.

(16) Bloomfield, V. A.; Crothers, D. M.; Tinoco, I., Jr. *Nucleic Acids: Structures, Properties, and Functions*; University Science Books: Sausalito, CA, 2000.

(17) (a) Okamoto, A.; Saito, Y.; Saito, I. *J. Photochem. Photobiol. C* **2005**, *6*, 108−122. (b) Okamoto, A. *Bull. Chem. Soc. Jpn.* **2005**, *78*, 2083−2097. (c) Okamoto, A.; Tainaka, K.; Ochi, Y.; Kanatani, K.; Saito, I. *Mol. BioSyst.* **2006**, *2*, 122−127.

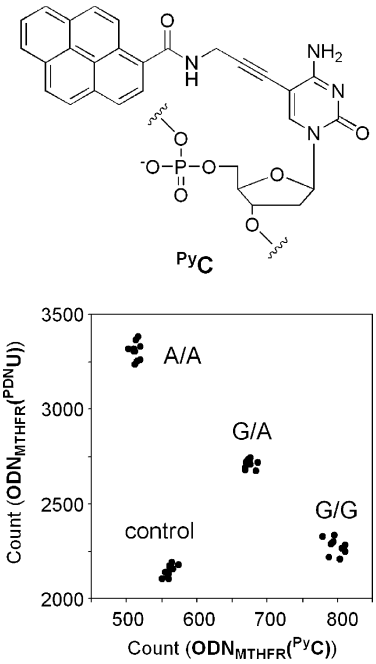

Figure 7. Structure of ^{Py}C and cluster diagram showing the genotype assignment for an hMTHFR C677T SNP in 25 samples using ^{PDN}U- and ^{Py}C-probes. The samples amplified by asymmetric PCR were added to a solution of 2.5 mM probes in a 50 mM sodium phosphate (pH = 7.0) and 100 mM sodium chloride on a 1536-well microtiter plate. Equipment used: a 440 ± 10 nm excitation band-pass filter and a 510 ± 10 nm emission band-pass filter for **ODN$_{MTHFR}$(^{PDN}U)**; a 340 ± 10 nm excitation band-pass filter and a 410 ± 5 nm emission band-pass filter for **ODN$_{MTHFR}$(^{Py}C)**; lamp energy = 7000 (× 75 × 2^{-16} W); count time = 0.1 s.

mentary strand (λ_{ex} = 329 nm, λ_{em} = 393 nm), whereas the fluorescence is very weak when ^{Py}C forms a base pair with A, C, or T.[3c] A mixture of probes that have different wavelengths of excitation and emission would enable the use of multicolored sensing of gene SNP sites. By addition of the mixture of ^{PDN}U- and ^{Py}C-labeled probes to a single well containing a gene sample, the type of base at a specific SNP site will be fluorometrically determinable in a single cuvette. Using ^{PDN}U- and ^{Py}C-containing BDF probes, we tested a BDF genotyping assay for a human methylenetetrahydrofolate reductase (hMTHFR) gene containing a C677T mutation, 5′-d(...ATGAAATCG-PCTC...)-3′ (P = G/A SNP site), which is associated with coronary artery disease.[18] We prepared BDF probes **ODN$_{MTHFR}$(B)** 5′-d(GAGBCGATTTCAT)-3′ (B = ^{PDN}U or ^{Py}C) for typing of an hMTHFR C677T SNP site. An SNP site containing a 109-nt fragment of the antisense strand of hMTHFR was amplified by asymmetric PCR and was added to a mixture containing both probes in 50 mM sodium phosphate (pH = 7.0) and 100 mM sodium chloride. The fluorescence from **ODN$_{MTHFR}$(^{PDN}U)** was detected through a 440 ± 10 nm excitation filter and a 510 ± 10 nm emission filter, and the fluorescence from **ODN$_{MTHFR}$(^{Py}C)** was detected through a 340 ± 10 nm excitation filter and a 410 ± 5 nm emission filter. When the fluorescence intensity of each probe was plotted on an $x-y$ plot, all the samples clearly separated into three clusters, which were identified as G-homozygotes, A-homozygotes, and heterozygotes (Figure 7). The SNP typing results obtained using the BDF method were in good agreement with those obtained by direct sequencing.

In conclusion, we have synthesized four PRODAN-labeled nucleosides ^{PDN}X and examined their photochemical properties. Their Stokes shift values significantly changed depending on the solvent orientational polarizability and DNA structure. ^{PDN}X fixed on a fully matched duplex exhibited an excitation spectrum at a longer wavelength and a smaller Stokes shift value, compared with those of ^{PDN}X in a single-stranded state and mismatched duplexes. The bathochromic shift of the excitation spectrum of ^{PDN}X and lower energy excitation resulted in fluorescence emissions selective to the Watson−Crick pairing base. The base-selective emission of ^{PDN}U facilitated multicolored SNP typing through the combination with BDF probes with a shorter emission wavelength. The photochemical property exhibited by PRODAN fixed on DNA is not only very unique but also applicable to the design of new fluorescent DNA probes for DNA sequencing, genotyping, monitoring of DNA structural transition, and observation of microenvironmental change attended by biomolecular interaction.

Experimental Section

General. NMR spectra were measured with Varian Mercury 400 and JEOL JNM-GX 400 spectrometers. Coupling constants (J value) are reported in hertz. The chemical shifts are shown in ppm downfield from tetramethylsilane, using residual chloroform (δ = 7.26 in ^{1}H NMR, δ = 77.0 in ^{13}C NMR) and dimethylsulfoxide (δ = 2.48 in ^{1}H NMR, δ = 39.5 in ^{13}C NMR) as an internal standard. FAB mass spectra were recorded on a JEOL JMS HX-110A spectrometer. Masses of ODNs were determined with a MALDI-TOF MS (Perseptive Voyager Elite, acceleration voltage 21 kV, negative mode) with 2′,3′,4′-trihydroxyacetophenone as a matrix, using T_8 ([M − H]$^-$ 2370.61) and T_{17} ([M − H]$^-$ 5108.37) as an internal standard for ODNs. Calf intestine alkaline phosphatase (Promega), *Crotalus adamanteus* venom phosphodiesterase I (USB), and *Penicillium citrinum* nuclease P1 (Roche) were used for the enzymatic digestion of ODNs.

6-Dimethylamino-2-(1-hydroxy-2-propyn-1-yl)naphthalene (2). To a solution of trimethylsilylacetylene (453 μL, 3.3 mmol) in THF (10 mL) was added *n*-butyllithium (1.6 M solution in hexane, 2.0 mL, 3.3 mmol) at −78 °C, and the reaction mixture was stirred at room temperature for 30 min. After addition of 6-dimethylamino-2-formylnaphthalene (500 mg, 2.5 mmol) in THF (20 mL) at −78 °C, the reaction mixture was stirred at 0 °C for 30 min. The resulting mixture was diluted with *sat. aq.* NH_4Cl at 0 °C, extracted with ethyl acetate. The organic phase was washed with brine, dried over anhydrous $MgSO_4$, filtered, and concentrated *in vacuo*. The crude product was purified by silica gel column chromatography (hexane−ethyl acetate = 5:1) to yield the adduct (683 mg, 2.3 mmol, 92%) as a yellow solid: ^{1}H NMR ($CDCl_3$, 400 MHz) δ 7.80 (s, 1H), 7.69−7.64 (m, 2H), 7.52 (dd, 1H, J = 1.7, 8.5 Hz), 7.15 (dd, 1H, J = 2.5, 9.1 Hz), 6.91 (s, 1H), 3.03 (s, 6H), 2.33 (brs, 1H), 0.21 (s, 9H); ^{13}C NMR ($CDCl_3$, 100 MHz) δ 148.9, 134.8, 133.9, 129.0, 126.8, 126.3, 125.4, 125.1, 116.6, 106.4, 105.3, 91.4, 65.3, 40.9, −0.1; FABMS (NBA/$CHCl_3$), m/z 297 (M^+), HRMS calcd for $C_{18}H_{23}ONSi$ (M^+) 297.1549, found 297.1550.

A mixture of the adduct (683 mg, 2.3 mmol) and sodium methoxide (100 mM in methanol, 20 mL) was stirred at room temperature for 1 h. The reaction mixture was neutralized with 1 M HCl and extracted with ethyl acetate. The organic phase was washed with brine, dried over anhydrous $MgSO_4$, filtered, and concentrated *in vacuo*. The crude product was purified by silica gel column chromatography (hexane−ethyl acetate = 3:1) to yield **2** (500 mg, 2.2 mmol, 97%) as a yellow syrup: ^{1}H NMR ($CDCl_3$, 400 MHz) δ 7.85 (s, 1H), 7.72 (d, 1H, J = 9.0 Hz), 7.68 (d, 1H, J = 8.6 Hz), 7.54 (dd, 1H, J = 1.6, 8.4 Hz), 7.18

(18) (a) Girelli, D.; Friso, S.; Trabetti, E.; Olivieri, O.; Russo, C.; Pessotto, R.; Faccini, G.; Pignatti, P. F.; Mazzucco, A.; Corrocher, R. *Blood* **1998**, *91*, 4158−4163. (b) Brody, L. C.; Conley, M.; Cox, C.; Kirke, P. N.; McKeever, M. P.; Mills, J. L.; Molloy, A. M.; O'Leary, V. B.; Parle-McDermott, A.; Scott, J. M.; Swanson, D. A. *Am. J. Hum. Genet.* **2002**, *71*, 1207−1215.

(dd, 1H, J = 2.2, 9.0 Hz), 6.92 (s, 1H), 5.57 (s, 1H), 3.06 (s, 6H), 2.71 (d, 1H, J = 2.2 Hz), 2.25 (brs, 1H); ^{13}C NMR ($CDCl_3$, 100 MHz) δ 149.0, 134.9, 133.5, 129.0, 126.9, 126.3, 125.3, 124.9, 116.7, 106.3, 83.9, 74.6, 64.7, 40.8; FABMS (NBA/$CHCl_3$) m/z 225 (M^+), HRMS calcd for $C_{15}H_{15}ON$ (M^+) 225.1154, found 225.1150.

5-[3-(6-Dimethylaminonaphthalen-2-yl)-3-hydroxy-1-propyn-1-yl]-3′*O*,5′*O*-bis(*tert*-butyldimethylsilyl)-2′-deoxyuridine (3). To a solution of 5-iodo-3′ *O*,5′*O*-bis(*tert*-butyldimethylsilyl)-2′-deoxyuridine (2.9 g, 5.0 mmol), **2** (915 mg, 4.1 mmol), and triethylamine (1.7 mL, 12 mmol) in DMF (20 mL) were added tetrakis(triphenylphosphine)-palladium(0) (950 mg, 0.82 mmol) and copper(I) iodide (310 mg, 1.6 mmol) under nitrogen. The mixture was stirred at room temperature for 5 h. The resulting mixture was concentrated *in vacuo* and diluted with ethyl acetate. This solution was washed with 5% (w/v) EDTA solution and 5% (w/v) sodium bisulfite solution, dried over Na_2SO_4, filtered, and evaporated. The crude product was purified by silica gel column chromatography (toluene−ethyl acetate = 4:1) to yield **3** (3.2 g, 4.65 mmol, 93%) as a yellow solid: ^{1}H NMR ($CDCl_3$, 400 MHz) δ 8.59 (brs, 1H), 7.98 (d, 1H, J = 3.3 Hz), 7.88 (s, 1H), 7.71 (d, 1H, J = 9.0 Hz), 7.64 (d, 1H, J = 9.6 Hz), 7.56 (dd, 1H, J = 1.6, 8.5 Hz), 7.15 (dd, 1H, J = 2.5, 9.1 Hz), 6.90 (d, 1H, J = 2.0 Hz), 6.27 (dd, 1H, J = 5.8, 7.6 Hz), 5.73 (s, 1H), 4.39−4.37 (m, 1H), 3.97−3.96 (m, 1H), 3.85 (ddd, 1H, J = 2.6, 5.4, 11.4 Hz), 3.74−3.71 (m, 1H), 3.04 (s, 6H), 2.69 (brs, 1H), 2.30 (ddd, 1H, J = 2.5, 5.8, 13.1 Hz), 2.04−1.96 (m, 1H), 0.89−0.83 (m, 18H), 0.08−0.02 (m, 12H); ^{13}C NMR ($CDCl_3$, 100 MHz) δ 161.2, 149.0, 142.5, 134.9, 133.7, 129.1, 126.8, 126.43, 126.42, 125.52, 125.46, 125.12, 125.07, 116.6, 106.3, 99.6, 94.2, 88.4, 85.91, 85.88, 77.6, 77.5, 72.4, 65.3, 63.0, 42.0, 40.8, 25.9, 25.7, 18.3, 18.0, −4.8, −4.7, −5.4, −5.6; FABMS (NBA/$CHCl_3$) m/z 679 (M^+), HRMS calcd for $C_{36}H_{53}O_6N_3Si_2$ (M^+) 679.3473, found 679.3475.

5-PRODAN-3′*O*,5′*O*-bis(*tert*-butyldimethylsilyl)-2′-deoxyuridine (4). A mixture of **3** (673 mg, 0.99 mmol) and 10% Pd/C (180 mg) in methanol (10 mL) was stirred under hydrogen atmosphere at room temperature for 9 h. The mixture was filtered through Celite, washed with methanol, and evaporated under reduced pressure. The crude product was purified by silica gel chromatography (hexane−ethyl acetate = 3:1) to yield the corresponding reduction product (diastereomeric mixture, 488 mg, 0.71 mmol, 72%) as a yellow solid: ^{1}H NMR ($CDCl_3$, 400 MHz) δ 8.41 and 8.40 (s × 2, total 1H), 7.67 (d, 1H, J = 9.0 Hz), 7.63 (s, 1H), 7.62 (d, 1H, J = 8.6 Hz), 7.431 and 7.428 (s × 2, total 1H), 7.37 and 7.34 (t × 2, total 1H, J = 1.8 Hz), 7.16 and 7.14 (d × 2, total 1H, J = 2.4 Hz), 6.904 and 6.898 (s × 2, total 1H), 6.30 (dd, 1H, J = 5.7, 8.1 Hz), 4.78−4.72 (m, 1H), 4.37 (dt, 1H, J = 2.6, 8.2 Hz), 3.92 (q, 1H, J = 2.5 Hz), 3.79 (ddd, 1H, J = 2.9, 4.4, 11.4 Hz), 3.72 (dt, 1H, J = 3.0, 11.4 Hz), 3.03 (s, 6H), 2.84 and 2.75 (brs × 2, total 1H), 2.56−2.41 (m, 2H), 2.222 and 2.216 (quintet × 2, total 1H, J = 2.6 Hz), 2.09−1.90 (m, 3H), 0.89 (s, 9H), 0.86 (d, 9H, J = 4.8 Hz), 0.08−0.02 (m, 12H); ^{13}C NMR ($CDCl_3$, 100 MHz) δ 163.6, 163.5, 149.93, 149.89, 148.7, 137.84, 137.75, 136.21, 136.16, 134.5, 128.7, 126.6, 124.4, 124.3, 124.2, 116.7, 114.6, 106.5, 87.9, 84.99, 84.96, 73.4, 73.3, 72.41, 72.36, 63.1, 63.0, 41.2, 40.9, 38.39, 38.36, 25.90, 25.88, 25.7, 23.9, 23.8, 18.4, 18.0, −4.5, −4.8, −5.40, −5.43, −5.5; FABMS (NBA/$CHCl_3$) m/z 681 (M^+), HRMS calcd for $C_{36}H_{55}O_6N_3Si_2$ (M^+) 681.3629, found 681.3632.

To a solution of the previous reaction product (104 mg, 0.15 mmol) and molecular sieves (4 Å, 100 mg) in dichloromethane (4 mL) were added 4-methylmorpholine *N*-oxide (26.4 mg, 0.23 mmol) and tetrapropylammonium perruthenate (11 mg, 0.03 mmol) at 0 °C, and the mixture was stirred at room temperature for 1 h. After dilution with diethyl ether (10 mL), Florisil (60−100 mesh, 100 mg) was added to the solution and the resulting mixture was stirred at room temperature for 15 min. The mixture was filtered through Celite, washed with diethyl ether, and evaporated under reduced pressure. The crude product was purified by silica gel column chromatography (hexane−ethyl acetate = 4:1) to yield **4** (88 mg, 0.13 mmol, 85%) as a lemon yellow solid: ^{1}H NMR ($CDCl_3$, 400 MHz) δ 8.33 (s, 1H), 8.16 (brs, 1H), 7.90 (dd, 1H, J = 1.7, 8.7 Hz), 7.78 (d, 1H, J = 9.2 Hz), 7.63−7.59 (m, 2H), 7.16 (dd, 1H, J = 2.5, 9.1 Hz), 6.86 (d, 1H, J = 2.2 Hz), 6.31 (dd, 1H, J = 5.9, 7.7 Hz), 4.42 (dt, 1H, J = 2.7, 5.7 Hz), 3.94 (q, 1H, J = 3.0 Hz), 3.84 (dd, 1H, J = 3.6, 11.3 Hz), 3.78 (dd, 1H, J = 3.3, 11.2 Hz), 3.41−3.24 (m, 2H), 3.10 (s, 6H), 2.79 (t, 2H, J = 7.3 Hz), 2.23 (ddd, 1H, J = 2.7, 5.8, 13.1 Hz), 2.02 (ddd, 1H, J = 5.9, 7.7, 13.4 Hz), 0.92−0.90 (m, 18H), 0.11−0.07 (m, 12H); ^{13}C NMR ($CDCl_3$, 100 MHz) δ 198.3, 163.2, 150.2, 150.0, 137.6, 137.2, 130.7, 130.3, 130.0, 126.1, 125.1, 124.4, 116.3, 113.8, 105.3, 87.8, 84.9, 72.3, 63.1, 40.9, 40.4, 36.9, 25.9, 25.7, 22.7, 18.4, 18.0, −4.7, −4.8, −5.3, −5.4; FABMS (NBA/$CHCl_3$) m/z 682 ([M + H]$^+$), HRMS calcd for $C_{36}H_{56}O_6N_3Si_2$ ([M + H]$^+$) 682.3708, found 682.3704.

5-PRODAN-2′-deoxyuridine (5). To a solution of **4** (343 mg, 0.50 mmol) in THF (5 mL) was added tetrabutylammonium fluoride (1 M solution in THF, 1.1 mL, 1.1 mmol). The mixture was stirred at room temperature for 12 h. The resulting mixture was evaporated and purified by silica gel column chromatography (chloroform−methanol = 20:1) to yield **5** (186 mg, 0.41 mmol, 82%) as a lemon yellow solid: ^{1}H NMR (DMSO-d_6, 400 MHz) δ 11.4 (brs, 1H), 8.46 (s, 1H), 7.89 (d, 1H, J = 9.2 Hz), 7.82 (dd, 1H, J = 1.7, 8.7 Hz), 7.79 (s, 1H), 7.67 (d, 1H, J = 8.8 Hz), 7.27 (dd, 1H, J = 2.6, 9.2 Hz), 6.94 (d, 1H, J = 2.4 Hz), 6.17 (t, 1H, J = 6.9 Hz), 5.27 (brs, 1H), 5.09 (brs, 1H), 4.24 (m, 1H), 3.76 (q, 1H, J = 3.5 Hz), 3.61−3.53 (m, 2H), 3.27−3.22 (m, 2H), 3.05 (s, 6H), 2.57 (t, 2H, J = 7.6 Hz), 2.14−2.03 (m, 2H); ^{13}C NMR (DMSO-d_6, 100 MHz) δ 198.2, 163.4, 150.3, 150.1, 137.2, 136.7, 130.6, 129.9, 129.6, 125.9, 124.5, 123.8, 116.4, 112.7, 104.7, 87.3, 83.9, 70.3, 61.2, 39.9, 39.4, 36.6, 21.8; FABMS (NBA/DMSO) m/z 454 ([M + H]$^+$), HRMS calcd for $C_{24}H_{28}O_6N_3$ ([M + H]$^+$) 454.1978, found 454.1978.

5-PRODAN-5′*O*-(4,4′-dimethoxytrityl)-2′-deoxyuridine 3′*O*-(2-cyanoethyl)-*N*,*N*-diisopropylphosphoramidite (6). To a solution of **5** (166 mg, 0.40 mmol) in pyridine (5 mL) was added 4,4′-dimethoxytrityl chloride (174 mg, 0.51 mmol). The mixture was stirred at room temperature for 4 h. The resulting mixture was evaporated and purified by silica gel column chromatography (ethyl acetate) to yield the tritylated product (278 mg, 0.37 mmol, 93%) as a lemon yellow solid: ^{1}H NMR (DMSO-d_6, 400 MHz) δ 11.39 (brs, 1H), 8.31 (s, 1H), 7.83 (d, 1H, J = 9.2 Hz), 7.71 (dd, 1H, J = 1.6, 8.6 Hz), 7.63 (d, 1H, J = 8.8 Hz), 7.53 (s, 1H), 7.36 (d, 2H, J = 7.5 Hz), 7.27−7.21 (m, 7H), 7.12 (t, 1H, J = 7.3 Hz), 6.93 (d, 1H, J = 2.4 Hz), 6.82 (d, 4H, J = 8.6 Hz), 6.22 (t, 1H, J = 6.8 Hz), 5.30 (d, 1H, J = 4.2 Hz), 4.32−4.27 (m, 1H), 3.88 (q, 1H, J = 3.8 Hz), 3.64 (s, 6H), 3.20 (d, 2H, J = 4.0 Hz), 3.05 (s, 6H), 3.03 (t, 2H, J = 7.7 Hz), 2.34−2.16 (m, 4H); ^{13}C NMR (DMSO-d_6, 100 MHz) δ 197.7, 170.2, 163.2, 158.1, 158.0, 150.2, 150.1, 144.6, 137.1, 136.4, 135.4, 135.3, 130.5, 129.7, 129.5, 127.8, 127.6, 126.6, 125.8, 124.5, 123.7, 116.3, 113.1, 113.0, 104.7, 85.7, 85.5, 83.9, 70.5, 63.8, 54.9, 39.9, 39.3, 36.8, 21.6; FABMS (NBA/DMSO) m/z 755 ([M + H]$^+$), HRMS calcd for $C_{45}H_{45}O_8N_3$ ([M + H]$^+$) 755.3207, found 755.3212.

To a solution of the tritylated compound (30.2 mg, 40.0 μmol) and tetrazole (3.08 mg, 43.7 μmol) in anhydrous acetonitrile (400 μL) was added 2-cyanoethyl tetraisopropylphosphorodiamidite (13.1 μL, 40.0 μmol) under nitrogen. The mixture was stirred at room temperature for 30 min. The mixture was filtered and used with no further purification.

ODN Synthesis and Characterization. ODNs were synthesized by a conventional phosphoramidite method by using an Applied Biosystems 392 DNA/RNA synthesizer. Commercially available phosphoramidites were used for dA, dG, dC, and dT. The crude mixture after phosphoramidite synthesis was used for ^{PDN}X. Synthesized ODNs were purified by reversed phase HPLC on a 5-ODS-H column (10 mm × 150 mm, elution with a solvent mixture of 0.1 M triethylamine acetate (TEAA), pH 7.0, linear gradient over 30 min from 5% to 30% acetonitrile at a flow rate of 3.0 mL/min). ODNs containing modified nucleotides were fully digested with calf intestine alkaline phosphatase

(50 U/mL), snake venom phosphodiesterase (0.15 U/mL), and P1 nuclease (50 U/mL) at 37 °C for 3 h. Digested solutions were analyzed by HPLC on a CHEMCOBOND 5-ODS-H column (4.6 mm × 150 mm), elution with a solvent mixture of 0.1 M TEAA, pH 7.0, flow rate of 1.0 mL/min. The concentration of each ODN was determined by comparing peak areas with a standard solution containing dA, dC, dG, and dT at a concentration of 0.1 mM. MALDI-TOF **ODN1(^{PDN}U)**: ([M − H]$^-$) calcd 4098.81, found 4098.23. **ODN2(^{PDN}U)**: ([M − H]$^-$) calcd 4128.83, found 4129.04. **ODN1(^{PDN}C)**: ([M − H]$^-$) calcd 4097.83, found 4097.97. **ODN1(^{PDN}A)**: ([M − H]$^-$) calcd 4121.85, found 4121.57. **ODN1(^{PDN}G)**: ([M − H]$^-$) calcd 4137.85, found 4137.95.

Fluorescence Spectra. The fluorescence spectra were obtained using a Shimadzu RF-5300PC spectrofluorophotometer at 25 °C using a cell with a 1 cm path length. The excitation and emission bandwidths were 1.5 nm.

The fluorescence quantum yield (Φ_F) was determined using 9,10-diphenylanthracene as a reference, with a known $\Phi_F = 0.95$ in ethanol. The area of the emission spectrum was integrated using the instrumentation software, and the quantum yield was calculated according to the following equation:

$$\Phi_{F(S)}/\Phi_{F(R)} = [A_{(S)}/A_{(R)}] \times [(\mathrm{Abs})_{(R)}/(\mathrm{Abs})_{(S)}] \times [{n_{(S)}}^2/{n_{(R)}}^2] \quad (1)$$

Here, $\Phi_{F(S)}$ and $\Phi_{F(R)}$ are the fluorescence quantum yields of the sample and the reference, respectively. The terms $A_{(S)}$ and $A_{(R)}$ are the areas under the fluorescence spectra of the sample and the reference, respectively; $(\mathrm{Abs})_{(S)}$ and $(\mathrm{Abs})_{(R)}$ are the optical densities of the sample and the reference solution at the wavelength of excitation, respectively; and $n_{(S)}$ and $n_{(R)}$ are the values of the refractive index for the solvents used for the sample ($n_{(S)} = 1.333$) and the reference ($n_{(R)} = 1.383$), respectively.

Melting Temperature (T_m) Measurements. All T_m's of the ODNs (2.5 μM, final duplex concentration) were measured in 50 mM sodium phosphate buffers (pH 7.0) containing 100 mM sodium chloride. Absorbance vs temperature profiles were measured at 260 nm using a Shimadzu UV-2550 spectrophotometer equipped with a Peltier temperature controller using a 1 cm path length cell. The absorbance of the samples was monitored at 260 nm from 5 °C to 90 °C with a heating rate of 1 °C/min. From these profiles first derivatives were calculated to determine the T_m value.

Multicolored SNP Typing. The amplification reaction of an MTHFR target DNA sample was performed using a BioRad MyCycler thermal cycler 96-well sample-loading tray. A 109-mer MTHFR gene antisense fragment containing a C677T site 5′-d(GCCTTCACAAAGCGGAAGAATGTGTCAGCCTCAAAGAAAAGCTGCGTGATGATGAAATCG(A/G)CTCCCGCAGACACCTTCTCCTTCAAGTGCTTCAGGTCAGCCTCAAAGC)-3′ (10 ng), Primer 1 5′-d(GCCTTCACAAAGCGGAA)-3′ (400 nM), and Primer 2 5′-d(GCTTTGAGGCTGACCTG)-3′ (400 nM) were added to 50 μL of the reaction mixture containing 7 U HotStarTaq DNA polymerase and HotStarTaq master mix (Qiagen). The thermal cycling program consisted of an initial incubation at 95 °C for 15 min, followed by 40 cycles of 30 s at 95 °C, 30 s at 55 °C, and 60 s at 72 °C. After thermal cycling and subsequent cooling, 15 μL aliquots of the amplified DNA mixtures were used to carry out a second asymmetric PCR. Primer 1 (400 nM) and Primer 2 (80 nM) were added to 50 μL of a reaction mixture containing 7 U HotStarTaq DNA polymerase and HotStarTaq master mix (Qiagen). The thermal cycling program consisted of an initial incubation at 95 °C for 15 min, followed by 40 cycles of 30 s at 95 °C, 30 s at 55 °C, and 60 s at 72 °C. After thermal cycling and subsequent cooling, the amplified DNA was purified using Qiagen Min Elute. The DNA was mixed with 2.5 μM fluorescent probes 5′-d(GAGBCGATTTCAT)-3′ (B = ^{PDN}U or ^{Py}C) in a buffer solution (pH = 7.0) consisting of 25 mM sodium phosphate and 50 mM sodium chloride at room temperature on a 1536-well microtiter plate, and the fluorescence was measured with a fluorescence reader (Berthold Mithras LB940). The fluorescence was measured through a 440 ± 10 nm excitation filter and a 510 ± 10 nm emission filter for the fluorescence from a ^{PDN}U probe and through a 340 ± 10 nm excitation filter and a 410 ± 5 nm emission filter for the fluorescence from a ^{Py}C probe. The count time was 0.1 s, and the lamp energy was 7000 ($\times 75 \times 2^{-16}$ W).

Acknowledgment. This research was supported by the Industrial Technology Research Grant Program in 2006 from the New Energy and Industrial Technology Development Organization (NEDO) of Japan.

Supporting Information Available: Detailed experimental data on the synthesis of ^{PDN}C, ^{PDN}A, and ^{PDN}G (PDF). This material is available free of charge via the Internet at http://pubs.acs.org.

JA069156A